A Polymeric Split Hopkinson Pressure Bar Instrumented with Velocity Gages

by D.T. Casem, W.L. Fourney and P. Chang

ABSTRACT—Polymeric split Hopkinson pressure bars are often used to test low-impedance materials at elevated strain rates. However, they tend to be viscoelastic, and a viscoelastic wave propagation model is required to analyze the data. This considerably complicates the analysis over the more common linear elastic split Hopkinson bar. In this research, a polymeric split Hopkinson bar is instrumented with electromagnetic velocity gages. The gages are placed at the interfaces between the bars and the specimen. By using this arrangement, viscoelastic effects in the bars are negligible and the need for a viscoelastic correction is eliminated. The method is applied by testing low-density foams.

KEY WORDS—split Hopkinson Bar, viscoelastic, bar wave dispersion, electromagnetic velocity gages

Introduction

Recently, there has been an increased interest in the development of high strain-rate testing techniques for low-impedance materials. Most of these techniques are based on the split Hopkinson pressure bar (SHPB), a widely accepted dynamic testing device capable of reaching strain rates on the order of 10^4 s^1. During a SHPB test, a specimen is compressed between two bars and its response is determined through measurements of stress waves in the bars. To use the SHPB effectively, the impedance of the bars should be "matched" to the specimen, i.e., to test a low-strength material low-impedance bars are often used. This can be accomplished through the use of polymeric bars. Unfortunately, polymeric bars tend to be viscoelastic, and one must be able to account for viscoelastic wave propagation in order to analyze the specimen. This complicates the analysis over the more common linear elastic SHPB, especially when the latter can be treated as non-dispersive.

Several authors have developed methods to characterize viscoelastic wave propagation and to apply them to the polymeric SHPB. Among the earliest and most complete of these is the work by Zhao and Gary[1,2] who generalized the Pochhammer–Chree equations to include linear viscoelastic material behavior and applied the results to nylon and acrylic bars. Viscous effects were included through the use of combined Maxwell–Voigt solids and, naturally, the theory accounts for attenuation and dispersion due to both material and geometry. Bacon[3] presented an empirical method to measure the dispersion and attenuation parameters directly, thus eliminating the need to determine a suitable system of spring/dashpot elements. This essentially extended the work of Lundberg and Blanc,[4] which did not include geometric dispersion. Still other corrections exist; see, for example, Sawas et al.[5]

It should be noted that the majority of the need for a viscoelastic correction pertains primarily to the propagation of waves within the bars. In fact, much of this need can be mitigated simply by reducing the distances between the specimen and the gages. This idea provides the impetus for the present paper, in which a polycarbonate SHPB is instrumented by placing electromagnetic velocity gages directly at the interfaces between the bars and the specimen. The advantage of this arrangement over the conventional strain gage arrangement is that viscoelastic effects in the bars can be neglected, i.e., the bars may be treated as if they are linear elastic. This is due to both the gage placement and through the direct measurement of velocity, and is true even in cases when the conventional strain gage configuration requires a viscoelastic analysis. Thus, the need for a reliable viscoelastic model is eliminated, as are the difficulties and shortcomings associated with these models.

Longitudinal Wave Propagation in Viscoelastic Bars

As mentioned above, the use of a polymeric SHPB in general requires a theory of viscoelastic wave propagation, although in some cases the linear elastic approximation of this theory may be adequate. The theory used herein is due to Bacon[3] and Lundberg and Blanc[4] and is summarized as follows. The bar material is represented by a frequency-dependent complex modulus of elasticity, $E(\omega)$. The one-dimensional wave equation, in frequency space, is then written

$$\frac{\partial^2 \hat{\varepsilon}(x, \omega)}{\partial x^2} = \gamma^2 \hat{\varepsilon}(x, \omega) \tag{1}$$

where the $\wedge$ denotes the Fourier transform. ε is axial strain and the term γ is called the *propagation coefficient*. It is related to E by

$$\gamma^2 = -\frac{\rho \omega^2}{E(\omega)} \tag{2}$$

where ρ is the density.

Dr. Daniel T. Casem (dcasem@arl.army.mil) (SEM Member) is a Research Engineer, U.S. Army Research Laboratory, AMSRL-WM-TD, Aberdeen, Proving Ground, MD 21005-5069, USA. Dr. William L. Fourney (SEM Member) is a Professor, Department of Aerospace Engineering, University of Maryland, College Park, College Park, MD 20742, USA. Dr. Peter Chang is an Associate Professor, Department of Civil Engineering, University of Maryland, College Park, College Park, MD 20742, USA.

Original manuscript submitted: May 1, 2001.
Final manuscript received: May 5, 2003.

The general solution of eq (1) is given by

$$\hat{\varepsilon}(x, \omega) = \hat{F}(\omega)e^{-\gamma x} + \hat{G}(\omega)e^{\gamma x} \tag{3}$$

where $\hat{F}(\omega)$ and $\hat{G}(\omega)$ represent wave trains that propagate in the directions of increasing and decreasing x, respectively. In general, a strain gage located at x would read the superposition of these two waves. However, in most applications with the SHPB, only one pulse is present at a gage at a given time so that $\hat{F}$ or $\hat{G}$ can be dealt with individually (i.e., one or the other may be treated as being zero). The primary concern is then the propagation of a pulse between the gage and some interface at a distance d from the gage. For example, if $G = 0$ and the gage is located at $x = 0$, stress and velocity at an interface at $x = d$ are determined from the measured strain gage, $\varepsilon_g(t)$, as follows:

$$\hat{\sigma}(d, \omega) = -\frac{\rho\omega^2}{\gamma^2}\hat{\varepsilon}_g(\omega)\, e^{-\gamma d} = E(\omega)\,\hat{\varepsilon}_g(\omega)\, e^{-\gamma d} \tag{4}$$

$$\hat{v}(d, \omega) = -\frac{i\omega}{\gamma}\hat{\varepsilon}_g(\omega)\, e^{-\gamma d}. \tag{5}$$

Thus, viscoelastic wave propagation can be dealt with provided γ is predetermined for the particular bar of interest. Practical methods for doing so are based on the comparison of the frequency components of an impulsive signal before and after it propagates along a bar.[3,4] In light of these methods, it is more convenient to view γ in terms of its real and imaginary parts:

$$\gamma(\omega) = \alpha + i\frac{\omega}{c}. \tag{6}$$

Here $\alpha(\omega)$ is an attenuation parameter that governs the attenuation of various frequency components as they propagate along the bar. Similarly, $c(\omega)$ gives the phase speeds of various frequency components that travel at different speeds due to viscous effects in the material. The net effect of this is that a transient pulse consisting of multiple frequency components disperses as it propagates. As mentioned above, it has also been shown by Bacon[3] that this measurement of phase speed also includes geometric dispersion effects that occur for signals whose wavelengths are comparable to the bar diameter (i.e., Pochhammer–Chree dispersion[6]). In other words, when $c(\omega)$ is empirically determined, the resulting phase speed contains the contribution to dispersion by both viscoelastic and geometric effects. Conversely, when $\alpha = 0$, the viscoelastic theory reduces to the linear elastic dispersion problem.[3,7]

At very low frequencies, attenuation is negligible and all frequencies are assumed to travel at the bar wave speed c_0 given by the static modulus E_0 according to $c_0 = \sqrt{E_0/\rho}$. This is the familiar non-dispersive linear elastic case in which pulses propagate along a bar without change in form. In this case, eqs (4) and (5) are replaced by

$$\sigma(d, t \pm d/c_0) = E_0\varepsilon_g(t) = \rho c_0^2\varepsilon_g(t) \tag{7}$$

$$v(d, t \pm d/c_0) = \pm c_0\varepsilon_g(t) \tag{8}$$

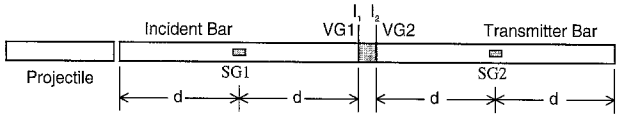

Fig. 1—The two SHPB systems discussed in this paper. The first is the conventional arrangement that uses only the strain gages (SG1 and SG2). The second system uses only the velocity gages (VG1 and VG2). I_1 and I_2 denote the interfaces between the specimen and the incident and transmitter bars, respectively.

where the quantity $\pm d/c_0$ accounts for the appropriate time shifting. The additional $\pm$ in eq (8) reflects the fact that the direction of the particle velocity depends on the direction of propagation (a tensile pulse produces particle motion in the opposite direction of propagation and a compressive pulse produces particle motion in the direction of propagation). Thus, non-dispersive, one-dimensional, linear elastic bar wave propagation can be treated completely knowing only c_0 and ρ.

Conventional Split Hopkinson Pressure Bar: Linear Elastic Case

The operation of the conventional linear elastic SHPB is well known[8–10] and is shown in Fig. 1 (ignore the velocity gages shown in the figure). A test sample is sandwiched between the incident and transmitter bars and the incident bar is struck with a projectile. The specimen is compressed and the resulting bar waves, the *incident*, *reflected*, and *transmitted* pulses, are monitored using strain gages at the mid-points of each bar. It is ensured that the pulses in the incident bar are short enough that they do not overlap at the gage and can be measured independently (this is one reason for the standard positioning of the gages at the mid-point).

Average specimen engineering stress (σ_S) and average engineering strain rate ($\dot{\varepsilon}_S$) are then determined by time-shifting the appropriate pulses to the instant at which they act at the specimen. In the simplest, linear elastic case, the equations are

$$\sigma_s = \sigma_{s2} = \frac{A_b}{A_s}E_0\varepsilon_T \tag{9}$$

$$\dot{\varepsilon}_s = -\frac{2c_0\varepsilon_R}{L_s} \tag{10}$$

where A_b and A_s are the initial cross-sectional areas of the bar and specimen, L_s is the initial specimen length, and ε_R and ε_T are the time-shifted strain signals for the reflected and transmitted pulses, respectively. Specimen strain is obtained from eq (10) by time integration.

The quantity σ_{s2} is used to denote the fact that eq (9) is really the specimen stress at the I_2 interface, as both eqs (9) and (10) assume that a state of equilibrium exists within the sample. Slightly more complicated equations are used if this is not the case. Conversely, it is possible to use the independent measurements of stress at each end of the specimen as a check of specimen equilibrium. In this situation, the specimen stress at I_2 is given by eq (9) and the specimen stress at

I_1 is given by

$$\sigma_{s1} = \frac{A_b}{A_s} E_0 (\varepsilon_I + \varepsilon_R) \tag{11}$$

where ε_I is the time-shifted incident pulse.

However, in many cases, the incident and reflected pulses, ε_I and ε_R, are not ideally suited to make an accurate stress measurement. For example, in the case of a very soft specimen, the magnitude of the reflected pulse is close to that of the incident pulse. As the signs of these pulses are opposite, poor resolution results when the two are added in eq (11). For this reason, most researchers use only the transmitted pulse to measure stress, and the incident bar is used only to measure the strain rate. This point will again be addressed below.

Conventional Split Hopkinson Pressure Bar: Linear Viscoelastic Case

The basic operation of the viscoelastic SHPB is essentially as described above, however the equations are developed from the viscoelastic theory. Specimen average engineering stress and strain rate are as follows:

$$\hat{\sigma}_{s2} (\omega) = -\frac{A_b}{A_s} \frac{\rho\omega^2}{\gamma^2} \hat{\varepsilon}_T e^{\gamma d} = E (\omega) \frac{A_b}{A_s} \hat{\varepsilon}_T e^{\gamma d} \tag{12}$$

$$\hat{\dot{\varepsilon}}_s = -\frac{2}{L_s} \frac{i\omega}{\gamma} \hat{\varepsilon}_R e^{\gamma d}. \tag{13}$$

As above, eq (12) is actually the specimen stress at the interface with the transmitter bar and both equations assume a state of specimen equilibrium. Similar to eq (11), the specimen stress at I_1 can be found by

$$\begin{aligned} \hat{\sigma}_{s1} (\omega) &= -\frac{A_b}{A_s} \frac{\rho\omega^2}{\gamma^2} \left(\hat{\varepsilon}_I e^{-\gamma d} + \hat{\varepsilon}_R e^{\gamma d} \right) \\ &= \frac{A_b}{A_s} E (\omega) \left(\hat{\varepsilon}_I e^{-\gamma d} + \hat{\varepsilon}_R e^{\gamma d} \right). \end{aligned} \tag{14}$$

In practice, the viscoelastic analysis is conducted in frequency space using the discrete fast Fourier transform (FFT) with digitized data, and the above equations are used somewhat indirectly as it is more convenient to perform the dispersion and attenuation operations on each pulse separately. However, the fundamentals are as above.

Split Hopkinson Pressure Bar Instrumented with Velocity Gages

The SHPB investigated during this research is also shown in Fig. 1. The interfaces between the bars and the specimen are instrumented with electromagnetic velocity gages (ignore the strain gages in the figure). The velocities of both ends of the specimen are therefore measured directly regardless of dispersion or attenuation. The specimen engineering strain rate is determined directly from these signals:

$$\dot{\varepsilon}_s (t) = \frac{-v_1(t) + v_2(t)}{L_s}. \tag{15}$$

Specimen stress is measured using the transmitter bar velocity gage, i.e., VG2 in the figure. Provided the test duration is sufficiently short that no reflections from the free end of the transmitter bar reach the gage, the transmitted pulse is measured directly at the specimen. Because of this, there is no need to account for dispersion or attenuation because the measurement is made exactly at the point of interest. All that remains is to determine the magnitude of the specimen stress. This is done by combining eqs (7) and (8) (letting $d = 0$ and eliminating ε_g) if the simple, non-dispersive, linear elastic theory is applied, and amounts to multiplying the measured particle velocity by the acoustic impedance of the bars and scaling by the relative cross-sectional areas of the bar and specimen. If the bars are viscoelastic, the relation is derived from eqs (4) and (5) instead. These equations reduce to

$$\sigma_{s2}(t) = -\rho c_0 \frac{A_b}{A_s} v_2(t) \tag{16}$$

$$\hat{\sigma}_{s2} (\omega) = -\rho \frac{\omega i}{\gamma} \frac{A_b}{A_s} \hat{v}_2(\omega). \tag{17}$$

The primary disadvantage of this method is that there is no way to measure the stress at the incident bar–specimen interface as is (at least theoretically) possible in the conventional arrangement. However, for the reasons discussed above, this is not usually a serious drawback. In cases when this is important, a technique involving pre-measurement of the incident pulse can be employed. This is discussed with the experimental results below.

Electromagnetic Velocity Gages

Basic Operation

The velocity transducer used in this research is the electromagnetic velocity gage. The gage, as shown in Fig. 2, is nothing more than a thin wire embedded diametrically through the bar. This embedded portion, dashed in the figure, is the gage. A uniform magnetic field of magnitude B is superimposed with a set of Helmholtz coils (not shown). The field lines are oriented such that they are perpendicular to both the axis of the bar and the gage. When a stress wave arrives, the bar and gage attain an axial velocity v. The gage crosses the magnetic field lines, and (by Faraday's law) an electric potential, E, is generated:

$$E = BvL. \tag{18}$$

Here L is the length of the gage, which, in this arrangement, is equal to the diameter of the bar. Lead wires extend from the gage so that the potential can be amplified and measured. Since the lead wires are parallel to the magnetic field, they do not cross any field lines when they move and therefore do not generate a signal. Although other configurations were attempted (conductive foils, wire loops, and various lead wire arrangements) that shown in Fig. 2 was determined the most practical for the SHPB.

Because the gages are so small (diameter <0.25 mm), they provide a simple, non-perturbing measurement of particle velocity with a high frequency response. They can also be placed very near the end of the bar (<2 mm). Furthermore, reasonable sensitivity can be achieved with a modest magnetic field (about 10 mT in these tests) and reasonable amplification (gains between 20 and 100). Increasing the field

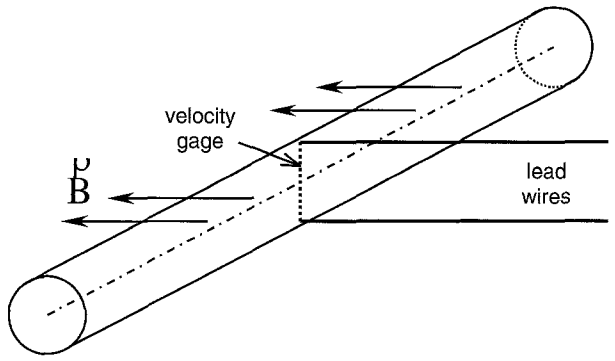

Fig. 2—A pressure bar with an electromagnetic velocity gage

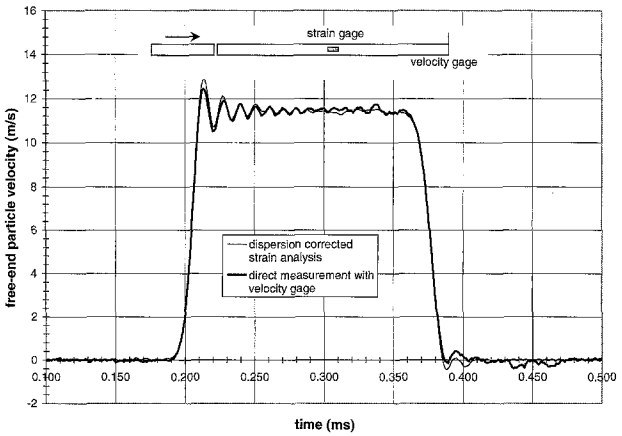

Fig. 3—Velocity at the end of an aluminum bar: direct measurement with velocity gage versus dispersion-corrected strain gage analysis

strength also increases sensitivity. It is also possible to increase L, although it is not very practical to increase the gage length much beyond the bar diameter.

Unfortunately, velocity gages have several disadvantages. The most restrictive of these is that they require a magnetic field to operate. This precludes their use on magnetic materials. Furthermore, the presence of the magnetic field may affect other instrumentation in the vicinity, and possibly even the specimen.

The greatest error source with these gages has to do with lead wire motion. As mentioned above, the motion of the lead wires does not create a signal provided they remain parallel to the magnetic field. However, as the gage moves, the lead wires move, and soon the lead wires are no longer parallel to the field. Even slight misalignment can result in considerable error because the lead wires are, in general, many times longer than the gage. It is possible to mitigate this error by preventing the leads from moving excessively. It was found that thick grease could be used to contain lead wire motion while still allowing them to move "freely" with the gage. In all cases discussed herein, the lead wires were passed through a mass of grease a few centimeters from the bar (not shown in the figure).

Calibration

Although other possibilities exist, the simplest way to calibrate the velocity gages in Fig. 1 involves measuring a known displacement. The bars are positioned with a precisely measured gap between them and the incident bar is impacted so that the gap closes. The calibration constant is then determined by correlating the known displacement to the integrated velocity signal. With this procedure, calibration constants between various tests are quite close, within $\pm 2\%$ of the average. It is expected that part of this error is due to uncertainty in the measurement of the initial gap.

Verification of Velocity Gage Data

To show the quality of the velocity data, Fig. 3 shows the free-end velocity of a 1219 mm long, 19.1 mm diameter aluminum pressure bar impacted by a similar projectile of length 425 mm. Two curves are shown. One is the velocity calculated from a strain gage located at the mid-point of the bar using the usual analysis, correcting for dispersion. The other is a direct measurement with a velocity gage. The closeness of the two traces is evident, with some discrepancy near the trailing end of the pulse. From this and similar experiments, it was concluded that the velocity gages are suitable for the research discussed herein.

Experimental Results

The following experimental results have been chosen to illustrate the necessity of using a viscoelastic analysis in the two SHPB configurations described above. For the sake of clarity, it should be emphasized that eqs (7)–(11) and (16) are nothing more than the zero frequency limits of their respective counterparts eqs (4), (5), (12)–(14) and (17). The latter group of equations includes dispersion and attenuation due to both geometry and attenuation, and from here on is referred to as the "viscoelastic" treatment. The former group of equations assumes a linear elastic material and neglects geometric dispersion, and is from here on designated the "elastic" treatment. The intermediate cases, where only viscoelastic effects or only geometric dispersion are considered, are not discussed.

When using the velocity gage technique, the only place where viscoelastic parameters arise is in the determination of specimen stress from measured velocity, eqs (16) and (17). It has been observed (see, for example, Zhao and Gary[2]) that locally, viscoelastic effects are insignificant and the distinction between these two equations is negligible. However, since eq (16) is the low-frequency approximation of eq (17), it is clear that this error increases at higher frequencies. It is therefore interesting to quantify the difference between the two as a function of frequency in an attempt to determine at what point the error becomes important. We can do this by considering the propagation coefficient for this system. The bars are made of polycarbonate with diameters of 19.1 mm and lengths of 1219 mm. The parameters $\alpha(\omega)$ and $c(\omega)$ were established using the methods of Bacon[3] and are shown in Fig. 4. The experimentally determined data have been extrapolated for the purpose of the following theoretical analysis. (The data are extrapolated because propagation data are very difficult to determine at high frequencies. By doing so, frequencies as high as 40 kHz can be considered in the analysis, even though they are not observed in actual experiments.)

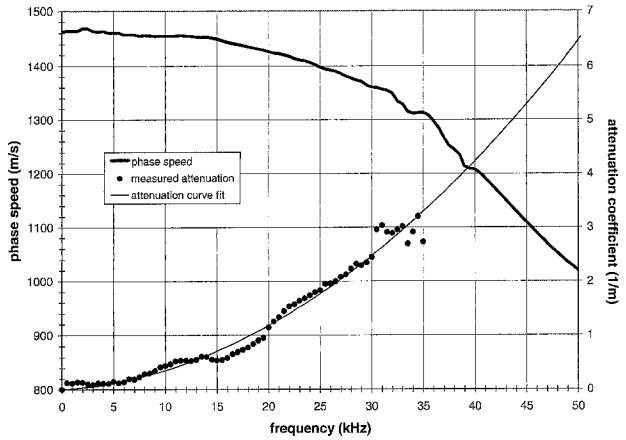

Fig. 4—Attenuation coefficient and phase speed for the 19.1 mm diameter polycarbonate bar used in this paper. The data are extrapolated beyond 35–40 kHz with a parabolic curve fit and the Pochhammer–Chree dispersion relations, respectively

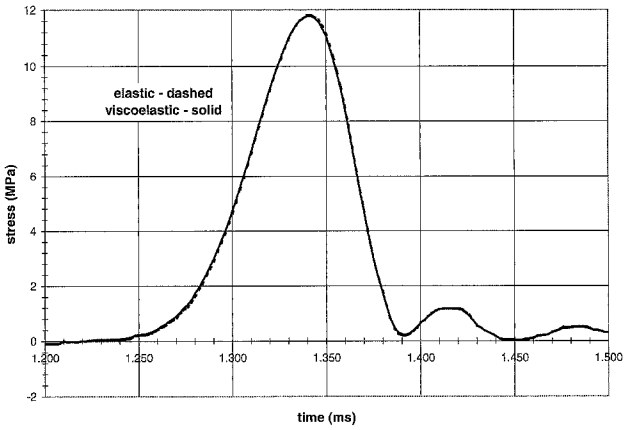

Fig. 6—Stress calculated from measured particle velocity using the elastic and viscoelastic solutions. The stress is positive in compression

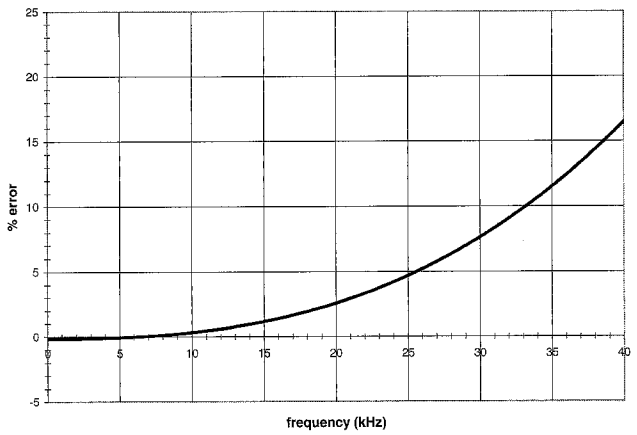

Fig. 5—Error associated with using the linear elastic approximation (eq (16)) to the more exact viscoelastic equation (eq (17)) when calculating stress from measured particle velocity

Using these data, the calculated magnitudes of stress from eqs (16) and (17) can be compared as a function of frequency. This is done in Fig. 5. The curve shows the error associated with approximating the full viscoelastic treatment with the simple linear elastic treatment when calculating stress from velocity measured at the point of interest. At low frequencies, the error is negligible, but becomes increasingly significant as the signal frequency increases. However, it remains quite small up to about 20–30 kHz, depending on the accuracy required. During practical testing, frequencies higher than this are rarely observed and almost never important, and in fact begin to violate the standard assumption that plane cross-sections of the bars remain plane throughout the deformation (for these bars, a wavelength of two bar diameters corresponds to a frequency of 34 kHz). Thus, in terms of practical applications, the elastic approximation is valid.

Impulsive Transient Signal

To elaborate this point, consider the following experiment. A short polycarbonate projectile (21 mm in length, 18 mm in diameter) impacts a polycarbonate pressure bar (1219 mm in length, 19.1 mm in diameter) at 14 m s^{-1} and generates an impulsive stress wave that propagates along the bar. The resulting axial particle velocity is measured by a velocity gage located at the mid-point of the bar. Using the propagation data of Fig. 4, the stress at this point can be determined from the measured velocity data with either the elastic or viscoelastic analysis, i.e., eqs (16) or (17). The results from both methods are plotted in Fig. 6, although the two curves are difficult to distinguish. Obviously, the viscoelastic analysis is unnecessary in this case.

This example can be used to establish the validity of the elastic approximation on actual polycarbonate pressure bar data. As discussed above, viscoelastic effects become more important as signal frequency increases. Depending on the desired degree of accuracy, we might make a decision based on the frequency spectrum of a given pulse and Fig. 5 as to when the simple elastic solution may be applied in place of the more complicated viscoelastic solution. However, in doing so, consideration should be given to the relative magnitude of the higher frequency components. In other words, although a particular signal may contain measurable components in the high-frequency range, they may not be (and often are not) significant to the construction of the entire signal. Considering the transient pulse above, in very few practical applications with a viscoelastic SHPB would a more impulsive signal be necessary (its length is about three bar diameters). The magnitude of the FFT of this signal shows that although frequencies in the range of 20–30 kHz are present, they are hardly significant. Therefore, the elastic approximation is an appropriate choice and good results (Fig. 6) are obtained.

Application: High Strain Rate Testing of Low-Density Foam

As stated above, the advantage of the velocity gage SHPB over the conventional strain gage SHPB is that viscoelastic effects in the bars can be neglected. To demonstrate this, the SHPB shown in Fig. 1 was used to test several low-density foam materials. The two configurations here provide a comparison between the two methods. The first configuration is

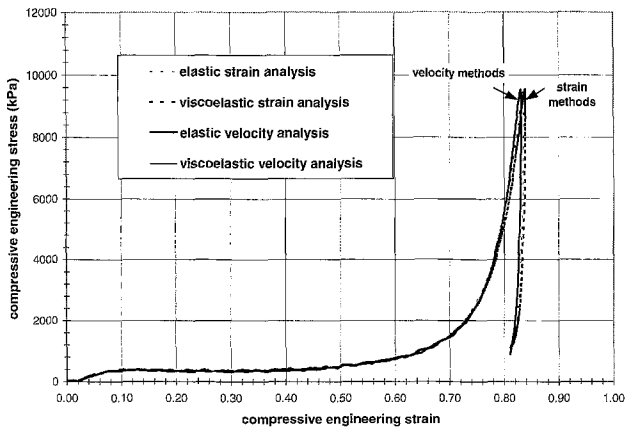

Fig. 7—Stress–strain curves obtained by the elastic and viscoelastic analyses for both the strain gage method and the velocity gage method (low-rate test). The viscoelastic correction is not needed in either case

the common strain gage arrangement. Using the strain data, the specimen may be analyzed using either an elastic or viscoelastic analysis (eqs (9) and (10), or eqs (12) and (13)). Similarly, data gathered using the velocity gages can be analyzed using an elastic or viscoelastic analysis (eqs (15) and (16), or eqs (15) and (17)). By comparing stress–strain curves from the four methods, the necessity of the viscoelastic correction in each case can be evaluated.

Low Strain Rate Test

At low strain rates viscoelastic corrections are often unnecessary. This is because the pulses generated during the tests do not contain a significant high-frequency spectrum. This is true for either method of instrumentation. For example, consider a test on a low-density foam at a strain rate of approximately 1500 s^{-1} (specimen length of 6.4 mm, diameter of 18.9 mm, striker velocity of 22 m s^{-1}). The resulting four stress–strain curves are shown in Fig. 7. It is clear that the viscoelastic correction offers only a very minor improvement in the strain gage analysis (very difficult to detect in the figure) and essentially no improvement in the velocity gage analysis (impossible to detect in the figure). In other words, the bars may be treated as linear elastic in either case.

It is also interesting to compare the velocity gage results to the strain gage results in Fig. 7. In theory, both of these are "exact", in the context that dispersion and attenuation within the one-dimensional framework presented in eqs (1)–(8) are accounted for. Indeed they are in good agreement. Any differences are attributed to measurement error, as the two curves utilize data from two completely different sets of gages.

Intermediate Strain Rate Test

Figure 8 shows the results of a test on the same material at a strain rate of 2500 s^{-1} (specimen length of 6.5 mm, diameter of 18.8 mm, and a striker velocity of 28 m s^{-1}). In this case, it is important to apply the viscoelastic correction to the strain gage analysis. This is shown in Fig. 8(a). The neglect of viscoelastic wave propagation results in a higher plateau stress and a lower densification strain than the actual

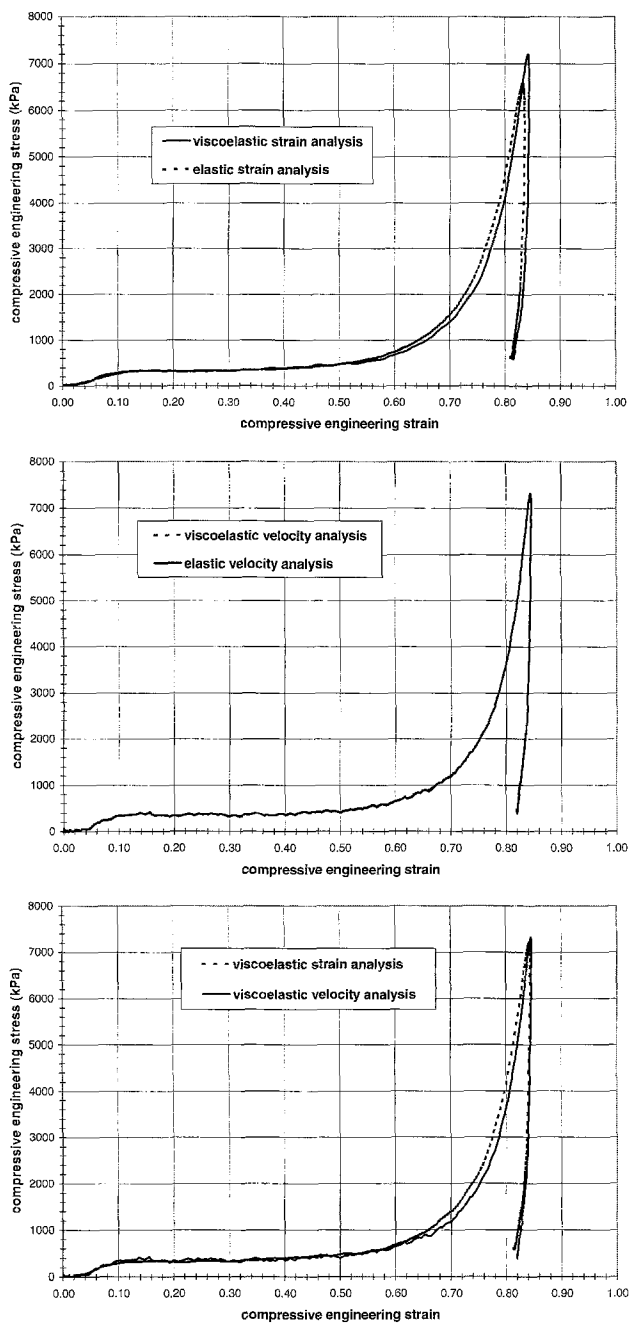

Fig. 8—Stress–strain curves for a foam sample at an intermediate strain rate. (a) Necessity of the viscoelastic correction for the strain gage analysis. (b) Necessity of the viscoelastic correction for the velocity gage analysis. (c) Comparison of the velocity gage method and the viscoelastic strain gage analysis

specimen response (given by the viscoelastic-corrected data). This demonstrates the danger of neglecting viscoelastic effects when using a polymeric pressure bar with the conventional strain gage arrangement. If viscoelastic effects were neglected, the incorrect stress–strain curve would be interpreted as a false strain rate hardening of the material.

Figure 8(b) shows the velocity gage results: the elastic compared to the viscoelastic. Again, no difference is observed, i.e., viscoelastic effects are negligible. Figure 8(c)

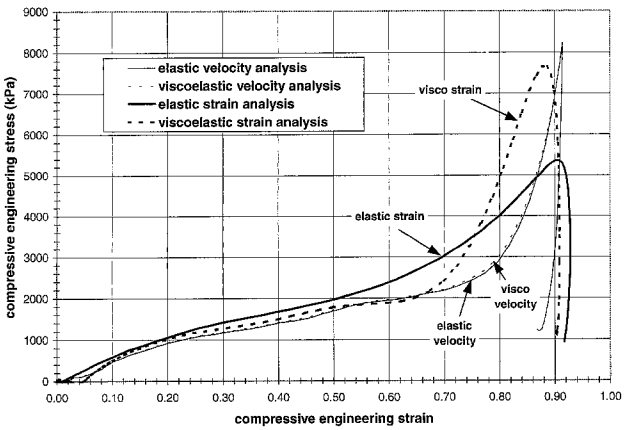

Fig. 9—Stress–strain curves obtained by the elastic and viscoelastic analyses for both the strain gage method and the velocity gage method at an extreme strain rate. The viscoelastic correction is negligible in the velocity gage analysis, and it fails to recreate the true stress–strain curve when applied to the strain gage analysis

shows the comparison between the viscoelastic strain gage analysis and the velocity gage analysis. Again, both should be exact, and indeed they are in good agreement.

High Strain Rate Test

As an extreme example, a test on another low-density foam was performed at approximately 10,000 s^{-1} (specimen length of 3.1 mm, diameter of 17.1 mm, and a striker velocity of 80 m s^{-1}). Although this may not be a valid test in terms of specimen equilibrium, it does illustrate several points about the methods. The results from the four analysis techniques are presented in Fig. 9. Considering the two strain gage analyses, clearly, there is an extreme difference between the two methods; the viscoelastic correction is absolutely necessary in this case. However, only a very minor difference can be observed in the velocity gage results. This small difference is arguably negligible and not worth correcting for, i.e., the simple elastic analysis is sufficient when the velocity gage method is applied.

It is also important to compare the velocity gage result to the corrected strain gage result. In theory, both should be exact, to the extent that the wave propagation is one-dimensional. However, the strain gage result, even though corrected for dispersion and attenuation, is in error. This is primarily due to the relatively high frequency content of the pertinent signals. The attenuation of these frequencies between the specimen and the gages is so great that they are reduced to immeasurable levels. Significant portions of the signals are therefore lost and the strain gage technique is unable to reconstruct the actual specimen response. This problem is exacerbated in the presence of electrical noise. If a noisy signal measured by a strain gage is dispersed to an earlier time (e.g., a transmitted or reflected pulse), the noise component is essentially amplified because the dispersion correction assumes that it is a part of the desired signal. When this is a problem, the only option is to filter the noise before the correction is applied. Because a portion of these components is part of the desired signal, the ability of the bars to faithfully carry these frequencies is compromised. The extent of these errors depends on several factors, such as the accuracy of the data acquisition system. However, in this research, they are suspected to be a notable source of error, even at more reasonable strain rates. They are, of course, altogether avoided by the velocity gage technique.

Measurement of Specimen Stress with the Incident Bar Velocity Gage

One disadvantage of the velocity gage method is that the stress at the interface between the incident bar and the specimen (I_1) cannot be determined directly without additional information. Additional gages on the incident bar can be used to provide this information, but the placement of these gages may require a full viscoelastic analysis.

Another method involves the measurement of the incident pulse before the test with the specimen. Without the transmitter bar in place, the incident bar is impacted with the striker at the same velocity that is to be used during the actual test. In this case, the velocity gage reads twice the incident pulse velocity, i.e.,

$$v_{1p}(t) = 2v_I(t). \tag{19}$$

The subscript "p" denotes the pre-test. Stress at I_1 can then be found after the test on the specimen from the difference between the pulses, in a fairly straightforward manner:

$$\sigma_{s1}(t) = -\frac{A_b}{A_s}\rho c_0 \left(v_{1p}(t) - v_1(t)\right). \tag{20}$$

The caveat here is that the accuracy of this technique depends on the repeatability of the incident pulse between the pre-test and the actual test. With striker bars, this is usually not a problem. However, use of other loading techniques (e.g., explosives and pulse shapers) will obviously depend on the controls of those systems.

An application of this technique is presented in Fig. 10. A test was conducted using the dual apparatus of Fig. 1 with a small gap left between the bars. When the incident pulse arrives at the I_1 interface, the gap begins to close (at about 1.70 ms). However, the interface remains stress-free until the instant it impacts the transmitter bar (at about 1.90 ms). Therefore, the expectation is that the stress on I_1 should be exactly zero up until the instant the gap closes and a square stress pulse is observed due to the impact of the bars. The stress is measured in two ways: (i) the standard strain gage analysis that involves the measurement of the incident and reflected pulses and the incorporation of a viscoelastic dispersion correction, eq (14), and (ii) the velocity gage method using a pre-measured incident pulse, eq (20). Both results show approximately what is expected, but the velocity technique is more accurate. The strain gage result contains oscillations that exist before the impact occurs even though the data are corrected for dispersion. This is due to errors in the dispersion correction, and is sometimes misinterpreted in actual tests as representing non-equilibrium effects within a specimen. (The dispersion corrected data do make a significant improvement over the uncorrected data.) The velocity gage technique avoids this correction entirely, and better results are obtained. However, it must be reiterated that this method depends entirely on the repeatability of the incident pulse between successive tests, and is therefore limited.

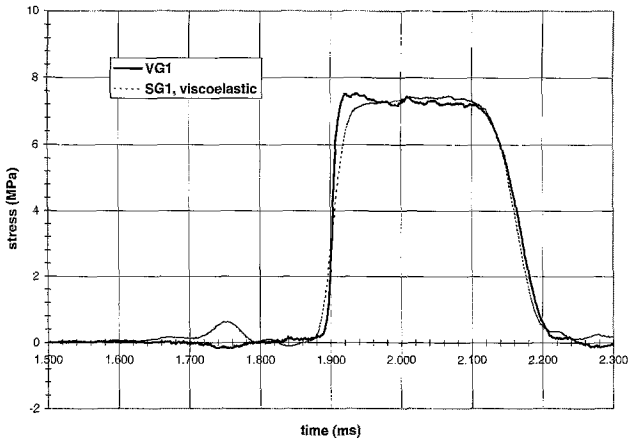

Fig. 10—Stress on the I_1 interface during a "gap" test: viscoelastic strain gage analysis versus pre-measured velocity gage analysis (elastic). The stress is positive in compression.

Discussion

As shown above, the main advantage of the velocity gage method over the conventional SHPB is that it avoids the need for a viscoelastic analysis. This is due primarily to the placement of the gages; no dispersion or attenuation occurs between the gages and the specimen. In terms of the calculation of stress from measured particle velocity, it was found that, in all cases with 19.1 mm diameter polycarbonate bars, the wave propagation is adequately described as being non-dispersive and linear elastic. Therefore, the only material properties necessary are the bar wave speed and the density; the propagation coefficient is unnecessary. In addition, none of the analysis is conducted in frequency space. Aside from simplifying calculations, this fact facilitates data acquisition. In order to apply a viscoelastic correction, we must ensure that the time window and vertical scaling are such that the entire signal is captured, even though the majority of this window is beyond the window of interest. The arrival of unwanted reflections also complicates the procedure. Neither of these are issues with the velocity gage method.

It is important to emphasize that much of the error due to the neglect of viscoelastic effects in the strain gage method is due to attenuation and dispersion between the gages and the specimen, and that simply placing the gages closer to the specimen can reduce this error. The basic limitation with strain gages is that the gages on the incident bar must be distant from the specimen so that the incident and reflected pulses can be measured independently. Furthermore, there is some question as to how close strain gages may be placed to the specimen interface so that measurements of surface strain accurately represent average strain over the cross-section. Nonetheless, it is certainly possible to configure a polycarbonate SHPB with strain gages positioned such that viscoelastic effects are negligible. The difficulty here is determining the minimum allowable distance between the gage and the specimen before viscoelastic effects become significant. This is easier to justify in the velocity gage case because a graph such as Fig. 5 can be used to describe the error in terms of signal frequency. Otherwise, there is nothing inherently wrong with measuring strain. In fact, it can be shown that errors similar to Fig. 5 exist when calculating stress and/or particle velocity from measured strain provided those calculations are made at the measurement point. (This fact is more or less routinely used by many users of viscoelastic SHPBs, i.e., viscoelastic corrections are used only to account for dispersion and attenuation of the strain signal, and not for the calculation of interface stress and velocity.) Similar statements apply to other transducers, e.g., pressure, force, acceleration.

One final advantage of the velocity gage technique is that it provides an extended test duration. The duration of the conventional SHPB is limited by the "length" of the incident pulse, which is limited to the length of the incident bar due to the need to independently measure the incident and reflected pulses by the gage at the mid-point. Referring to Fig. 1, the test duration is approximately $2d/c_0$. The velocity gage method is limited in duration by the time needed for the reflection of the transmitted pulse to arrive at the transmitter bar velocity gage (VG2). Thus, the time available for the test is doubled to $4d/c_0$ without the need for a wave separation technique. There is also no restriction on the projectile length, material, or shape.

As a final note, this discussion is limited to polycarbonate bars with 19.1 mm diameters. Although it may seem unlikely, other materials that exhibit greater viscoelastic behavior or bars of different diameter might not behave in this fashion. Other polymeric pressure bar systems should be evaluated on an individual basis.

Acknowledgments

This work was sponsored by the General Motors Corporation under a grant entitled "Material Characterization of Foam, Plastic and Glazing".

References

1. Zhao, H. and Gary, G., "A Three-Dimensional Analytical Solution of the Longitudinal Wave Propagation in an Infinite Linear Viscoelastic Cylindrical Bar. Application to Experimental Techniques," Journal of the Mechanics and Physics of Solids, **43** *(8), 1335 (1995).*

2. Zhao, H., Gary, G. and Klepaczko, J.R., "On the Use of a Viscoelastic Split Hopkinson Bar," International Journal of Impact Engineering, **19**, *319–330 (1997).*

3. Bacon, C., "An Experimental Method for Considering Dispersion and Attenuation in a Viscoelastic Hopkinson Bar," EXPERIMENTAL MECHANICS, **38**, *242 (1998).*

4. Lundberg, B. and Blanc, R.H., "Determination of Mechanical Material Properties from the Two-Point Response of an Impacted Linearly Viscoelastic Rod Specimen," Journal of Sound and Vibration, **126** *(1), 197 (1988).*

5. Sawas, O., Brar, N.S. and Brockman, R.A., "Dynamic Characterization of Compliant Materials Using an All-Polymeric Split Hopkinson Bar," EXPERIMENTAL MECHANICS, **38**, *205 (1998).*

6. Follansbee, P.S. and Franz, C., "Wave Propagation in the Split Hopkinson Pressure Bar," Transactions of the ASME: Journal of Engineering Materials and Technology, **105**, *61 (1983).*

7. Gorham, D.A. and Wu, X.J., "An Empirical Method for Correcting Dispersion in Pressure Bar Measurements of Impact Stress," Measurement Science and Technology, **7**, *1227 (1996).*

8. Meyers, M., Dynamic Behavior of Materials, Wiley, New York (1994).

9. Follansbee, P.S., Metals Handbook, Vol. 8, American Society for Metals, Metals Park, OH, 198 (1985).

10. Davies, R.M., Philosophical Transactions of the Royal Society of London, Series A, **240**, *375 (1948).*